

⁸B. N. Harmon and A. J. Freeman, *Phys. Rev. B* **10**, 1979, 4849 (1974); B. N. Harmon, private communication.

⁹Spin-orbit and exchange operators do not commute; hence spin is no longer a good quantum number. Spin-orbit effects generally lift the degeneracies of majority- and minority-spin bands.

¹⁰See Ref. 2 for a good review of the work by Freeman, Watson, and Dimmock, and other workers. See also the original papers by C. Jackson, *Phys. Rev.* **178**, 949 (1969) (Tb); S. C. Keeton and T. L. Loucks, *Phys. Rev.* **168**, 672 (1968) (Gd, Dy, Er, Lu); R. W. Williams, T. L. Loucks, and A. R. Mackintosh, *Phys. Rev. Lett.* **16**, 168 (1966) (Ho).

Direct Observation of Superlattice Formation in a Semiconductor Heterostructure

R. Dingle, A. C. Gossard, and W. Wiegmann
Bell Laboratories, Murray Hill, New Jersey 07974
 (Received 17 March 1975)

We demonstrate, via low-temperature optical-absorption measurements on ultrathin, coupled potential wells in molecular-beam-grown $\text{Al}_x\text{Ga}_{1-x}\text{As}$ -GaAs heterostructures, the evolution of resonantly split discrete well states into the lowest band of a one-dimensional superlattice. Both electron and hole superlattices appear to be practical.

The evolution of molecular-beam epitaxy¹ as a technique for the growth of ultrathin layers of high-quality III-V-semiconductor single crystals has allowed access to a new regime of quantum effects in structures approaching atomic dimensions. Quantum states of electrons^{2,3} and holes² in single potential wells of GaAs bounded by thick $\text{Al}_x\text{Ga}_{1-x}\text{As}$ barriers have been observed in tunneling³ as well as in optical absorption² and stimulated emission.⁴ Coupling between wells through thin penetrable barriers is expected to split the bound quantum states⁵ into symmetrical and anti-symmetrical combinations.⁶ In the limit of superlattice formation, multiple energy gaps occur in the Brillouin zone, and new and useful transport properties are anticipated. Tunneling measurements in AlGaAs-GaAs superlattices have been reported,⁷ although effects due to the bound-state energy-level splittings caused by the coupling of the wells were not resolved, nor was evidence for tunneling via, or the splitting of, valence-band bound-hole states presented in the tunneling reports.^{3,7}

In this Letter, we report optical-absorption measurements in GaAs- $\text{Al}_x\text{Ga}_{1-x}\text{As}$ heterostructures that give clear evidence of the coupling of both hole and electron states in closely spaced potential wells, as well as showing a number of hitherto unobserved features of superlattice band formation. This work constitutes the first detailed study of the optical characteristics of a finite superlattice. By monitoring the evolution of the GaAs absorption spectrum as the number of

coupled wells is increased from one to ten, we are able to present unequivocal evidence for the tunneling of electrons and holes through the $\text{Al}_x\text{Ga}_{1-x}\text{As}$ barriers. Structures with ten or more coupled wells appear to approximate the superlattice regime, whereas structures with fewer wells are well described in terms of interacting single wells. The experimental data are interpreted with an exact solution of the Schrödinger equation for transmission through multiple rectangular potential barriers.

A series of structures, with GaAs well widths in the range $50 \text{ \AA} < L_z < 200 \text{ \AA}$ and $\text{Al}_x\text{Ga}_{1-x}\text{As}$ barrier widths in the range $12 \text{ \AA} < L_B < 18 \text{ \AA}$ (8–12 monolayers), were grown by molecular-beam epitaxy on GaAs substrates with use of a previously outlined procedure.² Al concentrations in the range from $x = 0.19$ to 0.27 were studied. At our present growth rate, the barriers could be reproducibly grown in 3 or 4 sec. Thick layers grown under identical circumstances on semi-insulating substrates were low-doped p type.² Handling subsequent to growth included etching, mounting, cooling ($< 2 \text{ K}$), and spectral measurements as previously reported.² For the absorption measurements the beam passed normal to the layers.

The relevant barrier and well thicknesses were determined by interference-microscope measurement of total growth thickness in combination with Al-content determination by interband-absorption-edge and growth-time details. This Al-content determination was also used to establish

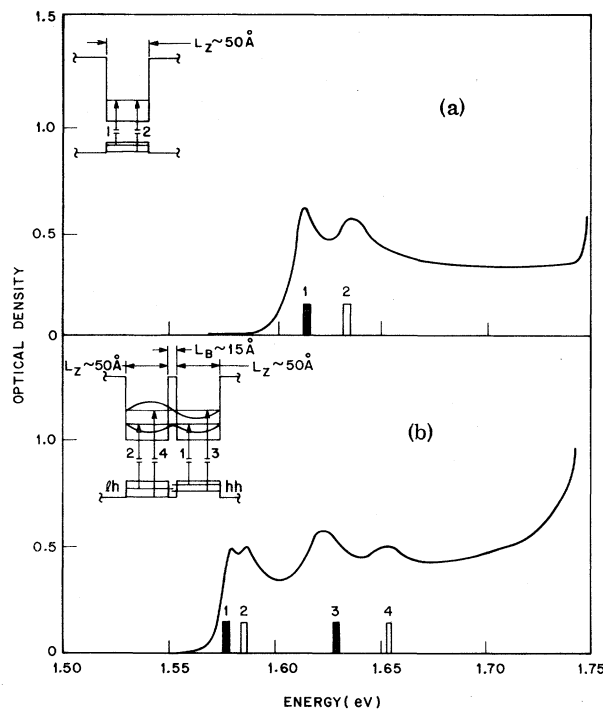


FIG. 1. (a) Optical-density spectrum of a series of eighty single GaAs wells isolated by thick ($\sim 180 \text{ \AA}$) $\text{Al}_{0.27}\text{Ga}_{0.73}\text{As}$ barriers. Peaks 1 and 2 correspond to exciting an electron from $n=1$ heavy-mass and light-mass valence-band bound states, respectively, to the $n=1$ conduction-band bound state, as shown in inset. Calculated predictions of peak positions for rectangular wells, based on growth parameters, are shown on abscissa. Black bars refer to heavy holes, white bars to light holes. (b) Spectrum of a series of sixty double GaAs wells coupled through thin ($\sim 15 \text{ \AA}$) $\text{Al}_{0.19}\text{Ga}_{0.81}\text{As}$ barriers. Both the $n=1$ hole and electron bound states are split by resonant coupling through the penetrable barriers, with symmetric (bonding) combinations of single-well states closest to the well bottoms. Each pair of wells is isolated from the adjacent pairs by 206 \AA of $\text{Al}_{0.19}\text{Ga}_{0.81}\text{As}$ barrier. Light- and heavy-hole states extend through both wells.

$\Delta E = E_g^{\text{Al}_x\text{Ga}_{1-x}\text{As}} - E_g^{\text{GaAs}} = \Delta E_{\text{CB}} + \Delta E_{\text{VB}}$. Values of $\Delta E_{\text{CB}}/\Delta E = 0.85 \pm 0.03$ and $\Delta E_{\text{VB}}/\Delta E = 0.15 \pm 0.03$ were used for the conduction-band and valence-band potential-barrier heights.² At the Al concentrations used, ΔE is proportional to x and equal to 250 meV at $x = 0.20$.

In Fig. 1(a) we present optical-absorption spectra (2 K) from a series of eighty rectangular GaAs wells of width $L_z = 50 \pm 2 \text{ \AA}$, interleaved by $\text{Al}_x\text{Ga}_{1-x}\text{As}$ layers $\sim 180 \text{ \AA}$ thick. At the operating temperature (2 K), tunneling of either bound holes or electrons through a barrier of this width is negligible. This structure thus corresponds

to the isolated-rectangular-well limit. The purpose of using eighty layers of GaAs is merely to enhance the total absorption in the structure.

The observed doublet at 1.615 and 1.637 eV is readily understood as the $\Delta n=0$,² heavy-hole ($n=1$), electron ($n=1$) transition and the light-hole ($n=1$), electron ($n=1$) transition, respectively. As previously pointed out,² the heavy hole corresponds to the valence band with dispersion in the k_z direction determined by the mass $(\gamma_1 - 2\gamma_2)^{-1} \times m_0 = 0.45 m_0$ and the light hole with $(\gamma_1 + 2\gamma_2)^{-1} \times m_0 = 0.08 m_0$. The bulk electron mass, $m_e = 0.0665 m_0$,³ is used throughout.

Calculated energies for these transitions with use of the above masses, with L_z from growth parameters, are shown as short vertical bars on the figure. The widths of the bars represent the distribution in absorption energies that would result from a distribution in L_z of ± 1 atomic layer ($\pm 1.4 \text{ \AA}$) with $\Delta E_{\text{CB}} = 0.85 \pm 0.03$. The agreement between theory and experiment is seen to be excellent and suggests uniformity among the layers of nearly monolayer precision. The essentially constant absorption to higher energies arises from states with higher transverse momenta. A relaxation time of $\sim 1 \text{ psec}$ is calculated from the linewidth of the lowest peak in the sharpest of our spectra. This is about an order of magnitude longer than electron-scattering times estimated from tunneling data.⁹

Coupled-well structures were produced by reducing the growth time of appropriate $\text{Al}_x\text{Ga}_{1-x}\text{As}$ barriers (every alternate barrier for a double-well structure for instance) while keeping the GaAs layer width constant. Extension to the superlattice regime is straightforward. We have examined coupled wells with a range of barrier widths down to $\sim 12 \text{ \AA}$. For the present study, narrow barriers have been chosen in a deliberate attempt to promote strong resonant coupling between identical states in closely juxtaposed wells. This strong coupling splits each single-well electron and hole quantum level into as many levels as there are coupled wells. This should lead to well-developed splittings *within* each $\Delta n = 0$ optical transition of the coupled-well spectrum. The observation of these splittings would satisfy the most stringent criterion for electron and hole tunneling through the $\text{Al}_x\text{Ga}_{1-x}\text{As}$ barriers.

The 2-K absorption spectrum of a double-well structure is shown in Fig. 1(b). This is an excellent example of the resonant splitting of degenerate single-well states into symmetric and

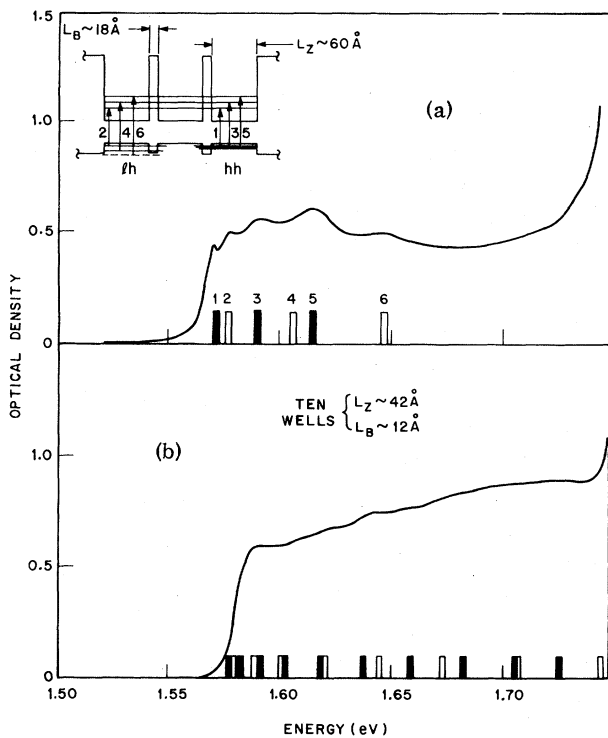


FIG. 2. (a) Triple-well optical-density spectrum. Barrier composition is $\text{Al}_{0.20}\text{Ga}_{0.80}\text{As}$. Increased absorption above 1.75 eV comes from interband absorption of buffer layers and barriers. Selection rules limit transitions to initial and final states with same interwell coupling symmetry. Sample contains forty triple wells. (b) Ten-well spectrum showing superlattice band formation. The $n=1$ level is split into ten levels, encompassing an approach to a band. Optical absorption is now extended across the entire $n=1$ bandwidth. Barrier is $\text{Al}_{0.27}\text{Ga}_{0.73}\text{As}$. Sample contains ten decawells.

antisymmetric combinations⁶ in the coupled-well limit. Although there are six coupled-well states within the $n=1$ manifold, inset Fig. 1(b), only four transitions appear because, in addition to the single-well selection rule $\Delta n=0$, an additional overlap rule, symmetric \rightarrow symmetric, antisymmetric \rightarrow antisymmetric, must be obeyed. The extension of this qualitative argument to three [Fig. 2(a)] or more coupled wells is straightforward. By the time ten wells are coupled together the spectrum is essentially devoid of recognizable structure [Fig. 2(b)]. The sharp lower absorption edge, together with the distribution of the calculated series of twenty closely spaced energy levels, indicates that this banding is not due to poor sample quality, but rather is due to the onset of superlattice behavior and miniband formation.

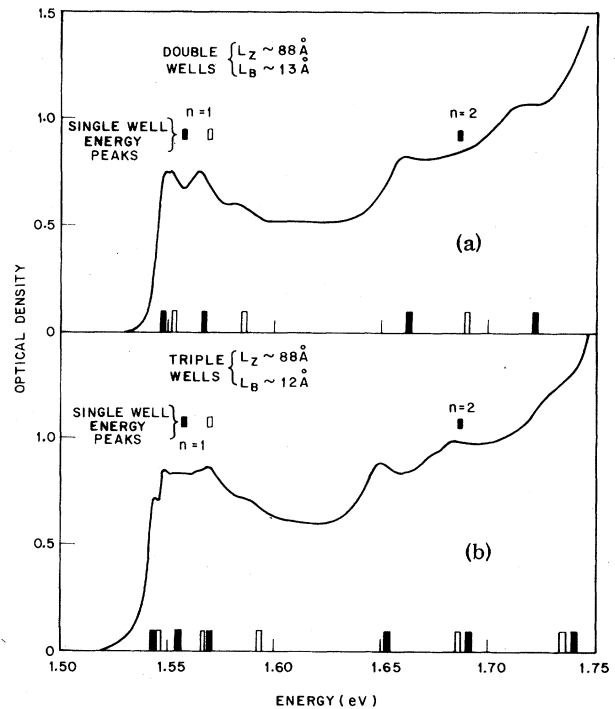


FIG. 3. (a) Double-well spectrum for wells sufficiently wide to contain both $n=1$ and $n=2$ bound states. Barriers are $\text{Al}_{0.23}\text{Ga}_{0.77}\text{As}$. Sample consists of 27 double wells. (b) Triple-well spectrum. Barriers are $\text{Al}_{0.20}\text{Ga}_{0.80}\text{As}$. Sample contains 22 triple wells.

In order to generate a theoretical fit to the observed absorption spectra of the coupled wells, the exact Schrödinger-equation solution for transmission through a series of rectangular barriers was used to find the energy levels of the bound particles. Peaks in the transmission coefficient of electrons (holes) impinging on the series of wells occur at the energies of the bound states. The particle transmission as a function of energy was computed for every sample by matching wave functions and first derivatives of wave functions at the interfaces.¹⁰ The theoretical absorption spectra were determined with use of the electron and hole energies obtained above and were corrected for exciton effects.² Remarkable agreement with experiment is obtained.

When structures with wider wells, $L_z \sim 90 \text{ \AA}$, capable of containing two bound-state levels were grown, optical-absorption spectra seen in Fig. 3 were obtained. Again, calculated spectra are in very good agreement with the experimental result, both within the $n=1$ and the $n=2$ manifolds of states, and development of the $n=1$ and $n=2$ bands can be seen.

In conclusion, our results confirm that series

of remarkably reproducible thin potential wells and barriers, essentially rectangular and uniform to the order of a monolayer, can be created with molecular-beam epitaxy. The coupling behavior of the wells proves that synthetic superlattices can indeed be created. The molecular-beam-epitaxy technique for fabrication and the optical technique for energy-level determination should be applicable to additional configurations and compositions of interest for both basic and applied studies.

We wish to acknowledge L. Kopf for the determination of the Al content of the layers and for expert technical assistance. We thank C. H. Henry and M. B. Panish for helpful discussions.

¹A. Y. Cho, Appl. Phys. Lett. **19**, 467 (1971).

²R. Dingle, W. Wiegmann, and C. H. Henry, Phys. Rev. Lett. **33**, 827 (1974).

³L. L. Chang, L. Esaki, and R. Tsu, Appl. Phys. Lett. **24**, 593 (1974).

⁴J. P. van der Ziel, R. Dingle, R. C. Miller, W. Wiegmann, and W. A. Norland, Appl. Phys. Lett. **26**, 463 (1975).

⁵R. Tsu and L. Esaki, Appl. Phys. Lett. **22**, 562 (1973).

⁶G. Herzberg, *Infrared and Raman Spectra of Polyatomic Molecules* (Van Nostrand, Princeton, N. J., 1962), p. 222.

⁷L. Esaki and L. L. Chang, Phys. Rev. Lett. **33**, 495 (1974).

⁸G. E. Stillman, C. M. Wolfe, and J. O. Dimmock, Solid State Commun. **7**, 921 (1969).

⁹L. Esaki, L. L. Chang, W. E. Howard, and V. L. Rideout, in *Proceedings of the Eleventh International Conference on the Physics of Semiconductors, Warsaw, Poland, 1972*, edited by The Polish Academy of Sciences (PWN—Polish Scientific Publishers, Warsaw, Poland, 1972), p. 431.

¹⁰We wish to thank G. A. Baraff for providing the computer program which we used to solve the Schrödinger equation for penetration of arbitrary well and barrier profiles.

Direct Measurement of One-Dimensional Plasmon Dispersion and Damping

J. J. Ritsko, D. J. Sandman, and A. J. Epstein

Xerox Webster Research Center, Webster, New York 14580

and

P. C. Gibbons, S. E. Schnatterly, and J. Fields

Princeton University, Princeton, New Jersey 08540

(Received 12 March 1975)

Plasmons in the one-dimensional organic metal tetrathiafulvalene-tetracyanoquinodimethane were directly measured by high-energy inelastic electron scattering in thin crystalline films at 300°K. For plasmons propagating along the conducting *b* axis the plasmon energy decreases from 0.75 to 0.55 eV and the width increases linearly as the plasmon momentum increases. Plasmons at 45° to *b* have an energy of 0.6 eV and show no dispersion.

The organic charge-transfer salt tetrathiafulvalene-tetracyanoquinodimethane (TTF-TCNQ) has been shown to have highly anisotropic electrical conductivity, and above 60°K has been characterized as a one-dimensional metal.¹ Since at high frequencies the room-temperature electronic behavior is certainly metallic in one dimension as established by the plasma edge reported in the normal-incidence reflectivity,²⁻⁴ TTF-TCNQ provides an opportunity to study the elementary excitations of a one-dimensional electron gas. We report here the first known *direct* measurements of plasmon dispersion and damping in such a material. The experiment, per-

formed at Princeton University, utilized high-energy inelastic-electron-scattering spectroscopy as the most sensitive and direct method to study dispersion and damping of plasma oscillations.

Epitaxial films of TTF-TCNQ (1000 Å thick) were grown on the (100) cleaved face of NaCl and had the same bioriented nature as previously observed.⁵ That is, the film consisted of irregularly shaped regions (20 μm across) within each of which the conducting *b* axis of the crystals pointed along one of the two orthogonal [110] directions in the face of the salt substrate. Our sample thus was equivalent to two TTF-TCNQ crystals at right angles to each other (both having the